Cold filtering of photons for a TES detector

Christina Schwemmbauer

Albert-Ludwigs University Freiburg

Germany

Supervision: Friederike Januschek and Axel Lindner

September 4, 2019

One of the main challenges of current dark matter experiments and searches are detection systems that require extremely low backgrounds. As such the Transition Edge Sensor (TES) used for single-photon detection in the ALPS II experiment has to tackle these challenges as well. ALPS II searches for Axion-Like-Particles (ALPs) with a Light-Shining-through-a-Wall (LSW) experimental setup and uses the Primakoff-like Sikivie effect to produce and detect ALPs, thus eliminating its dependency on theoretical models in comparison to e.g. helioscopes or haloscopes. The main background in the ALPs experiment is suspected to be the pile-up of black body radiation photons in a cryogenic environment. This work examines the possibility of using a broad bandpass filter to filter the low energy black body photons detected by the TES. Built into the cryostat is a filter bench manufactured for this purpose, which is supposed to enable single-photon detection for the ALPS II experiment. After conducting experiments on the behavior of the spectrum of the laser used for this setup in a warm and cold environment, it is evident that the influence of beam splitters, attenuators and mating sleeves on the spectrum needs to be further analyzed. The transmission of a laser beam through the filter was also tested in warm and cold environment and the filter showed all desired properties in being transparent to the laser light at the desired wavelength of 1064 nm. Furthermore the transmission through the filter bench needs to be improved further, since the influence of thermal shrinkage of the filter bench material accounts for a significant amount in transmission loss in the current setup.

Contents

1 Introduction

In the first Section, axions as well as the setup and working principle of the ALPS II experiment are shortly explained. Next, the need for filtering black body photons in the current setup will be motivated and the filter bench setup will be described. Finally different measurement methods are introduced, discussed and compared with expectations from theoretical calculations.

1.1 ALPs

Axions were first introduced in 1977 by Peccei & Quinn as a solution to the strong CP problem in QCD, posing one of the main inconsistencies of the current standard model of particle physics [1]. As such the axion belongs to the family of proposed particles called Weakly Interacting Sub-eV Particles (WISPs), which, as their name suggests, are of very small mass and only interact weakly with standard model particles. The peculiar name of the axion was chosen due to its possibility of "wiping out" the strong CP problem.

Furthermore the axion or similar particles called Axion-Like-Particles (ALPs) could also account for a considerable amount of cold dark matter. This is backed additionally by multiple astrophysical observations that can be explained through with existence of ALPs, such as the high flux of high energy gamma rays opposing predictions [3] and explain discrepancies between the luminosity of white dwarves and their models [4].

They can be detected via the Primakoff-like Sikivie effect as portrayed in Figure 1.

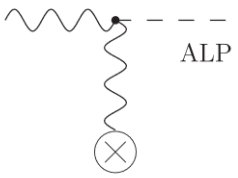

Figure 1: The Primakoff-like Sikivie effect shows photon-ALP-oscillation in the presence of a strong magnetic filed. Thus a photon, depicted as a wavy line, can theoretically be converted into an ALP. Picture from [5].

This effect is often used in Light-Shining-through-a-Wall (LSW) experiments searching for ALPs and WISPs. There the Sikivie effect is applied in order to detect ALPs, that have been created through photon-ALP-oscillation in front of a light tight wall and can pass this barrier due to their weak interaction.

1.2 The ALPS II experiment

The LSW experiment Any Light Particle Search (ALPS) II is the successor of the ALPS I experiment and involves the same detection principle i.e. using the Primakoff-like Sikivie effect. Although no WISPs or ALPs have been detected with the ALPS I experiment it was able to set constraints on the conversion probability of $\gamma \rightarrow \text{WISP} \rightarrow \gamma$ of $\sim 10^{-25}$ up to 5σ [6]. The ALPS II experiment has a similar setup as the ALPS I experiment described in [6] with some few significant changes. In the updated setup several superconducting HERA dipole magnets will be used and it will be assembled in a straight section in DESY's former HERA accelerator tunnel at HERA north. The schematic setup can be seen in Figure 2.

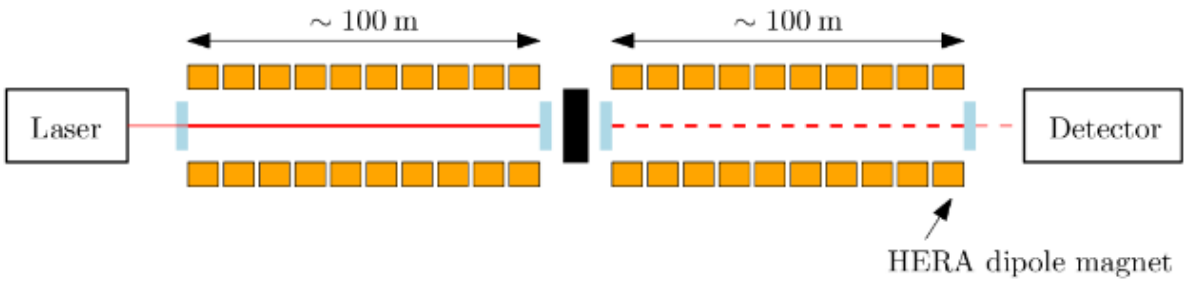

Figure 2: Setup of the ALPS II experiment. After recent discussion, an update from 20 to 24 straightened magnets is planned and will be installed in the setup. Figure from [2].

The number of magnets among other factors constrains the sensitivity for the detection of ALPs, since it is directly proportional to the effective magnetic field length ($B^2l^2 = (5.3\,\mathrm{T})^2 \cdot (125\,\mathrm{m})^2$). The capacity of the straight part of the HERA tunnel is reached with 24 magnets. With a 30 W laser system with infrared light of 1064 nm, explained in detail in [7], a laser field is produced in an optical cavity shown in the "left part" of the experiment in Figure 2. Through interaction of the laser field with virtual photons from the magnetic field permeating the cavity, ALPs can be generated through photon-ALP-oscillations. Due to this, the first resonant cavity is called the production cavity. This axion or ALP field can, radiating onward, pass the barrier or wall impenetrable for light; transparent for the weakly interacting axion field. There the axion or ALP field, enters another optical cavity held on resonance with the production cavity, where it couples back into a photon through the inverse Sikivie effect. Thus this cavity is called the regeneration cavity. Once a single photon is generated by this effect, and leaves this optical cavity, it is transferred to a single-photon detector via optical fibers. The Transition Edge Sensor (TES) used for this purpose will be explained in detail in the next section.

2 Filtering black body photons in a cryogenic environment

In this Section the difficulties accompanying the usage of a TES detector for single-photon signals at cryogenic temperatures will be discussed, including a short description of the working principles of TESs, the resulting problems for such a setup and possible solutions.

2.1 Transition Edge Sensors and the problem of black body radiation

The TES used for detecting reconverted photons in the ALPS II experiment is a tungsten microchip manufactured by NIST [8]. This TES is operated at ∼80 mK inside a BlueFors dilution refrigerator [9] referred to as cryostat or cryocooler in the following. The TESs working point is at the superconducting transition region at which the sensor's material transitions from superconductive to normal conduction properties, as can be seen in Figure 3.
When an incident photon reaches the tungsten chip with a critical temperature of $\sim T_\mathrm{C} \approx 140\,\mathrm{mK}$, on which some voltage is applied, its temperature rises by $\Delta T \approx 100\,\mu\mathrm{K}$. As can be seen in Figure 3 this yields an increase in resistance ΔR. As a consequence the TES gains normal ohmic resistance. The corresponding change in the current flowing through the TES causes a large magnetic flux change on the quantum scale, recognized by the SQUIDs (Superconducting QUantum Interference Device) which act as superconducting magnetometers.
In principle, a single photon originating from photon-ALP-oscillations at a wavelength of 1064 nm can be identified in this process. Detecting single-photons, however, is a challenging process that poses many difficulties due to low the low energies and low number of photons one has to deal with. Even

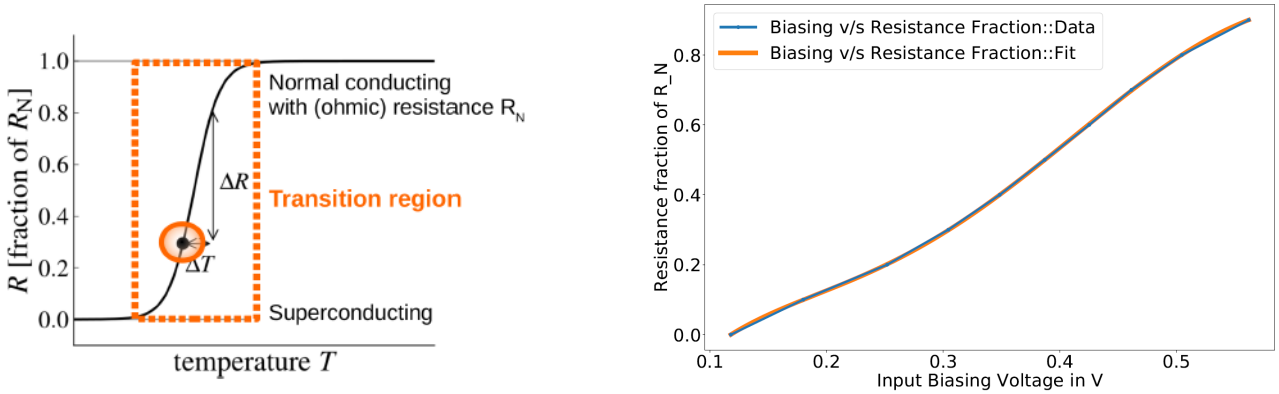

Figure 3: Left: Inside the orange dotted rectangle is the superconducting transition region of the TES. Beyond this region the tungsten chip shows normal conducting behavior and below it acts as a superconductor. In this transition edge, where the temperature is stabilized, small changes in temperature, e.g. coming from a single photon induce large changes in the resistance. Adapted from [2]. Right: Example for the transition region of the TES used in this setup. The plot shows the fraction of resistance achieved in relation to the input biasing voltage (aka heating). Plot by Rikhav Shah, internal communication 2019.

though the detection happens at temperatures as low as 80 mK, there has been detection of dark counts at 1064 nm possibly originating from pile-up of black body radiation. Even though it has been shown (see: [2]), that these dark counts have lower energies, pile-up due to the limited time-resolution of the TES imitates signals coming from 1064 nm photons.
Thus it is a primary goal for the ALPS TES detector to reduce the black body radiation background for ALPS II.

2.2 Filtering principle and setup

In order to reduce the effect of the pile-up, the idea is to install a filter in the system that filters black body photons before reaching the TES. For this a broadband bandpass interference filter by Edmund Optics is used. Its central wavelength is located at 1050 nm with a FWHM of 50 nm [10]. It should be able to reduce pile-up and be permeable for the desired 1064 nm photons. In order to include the filter in the setup, a titanium filter bench has been used with parts from Schäfter & Kirchhoff [11], the basic setup of this can be seen in Figure 4. The filter bench can then be mounted into the cryostat at the 40 K[1] stage of the cryocooler as can be seen in Figure 5.
One fiber going into the filter bench is coming from a 1064 nm laser diode beam source by Schäfter & Kirchhoff [11] coupled to a single mode fiber that is used to undertake tests on the filter. Usually the fiber leaving the filter then leads through the cryostat to the TES, although in this setup it leads out of the cryostat again for further testing. In the original setup the filter bench was employed with two titanium couplers. The process of aligning both couplers with respect to each other to gain maximum laser beam transmission is very delicate and demands high precision. Unfortunately one of the titanium couplers turned out to be defective between one of the following experiments. As a result it had to be replaced temporarily by a nickel-silver coupler with a higher thermal expansion coefficient. Thus, it is more sensitive to large temperature changes such as those inside the cryostat.

[1] Although in practice it goes down to 38 K.

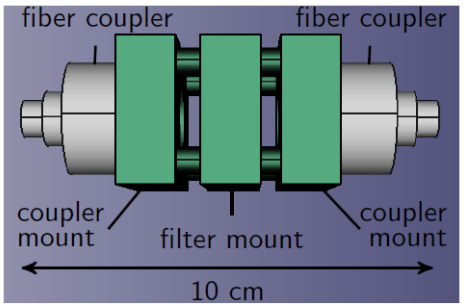

Figure 4: The filter bench setup consists of three titanium mounting plates (green) and two fiber couplers. The fiber couplers are made of amagnetic titanium in the original and presumably also in the future setup. The couplers are each placed on a coupler mount, whereas the filter can be inserted into the filter mount in the middle. The whole setup is kept tightly held in place by four metal rods. Titanium has been chosen due to its comparably low thermal expansion coefficient, resulting in relatively small material shrinkage while being inside the cryostat at the 40 K. Drawing from [12].

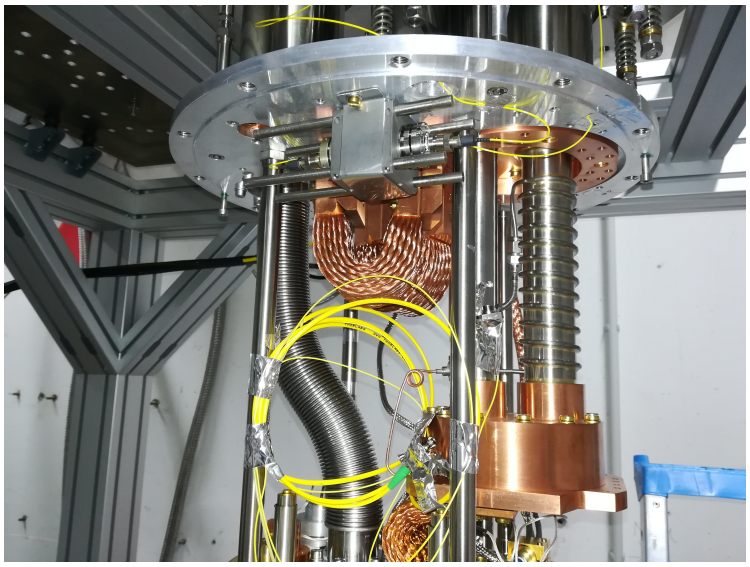

Figure 5: The filter bench inside of the opened cryostat fixed to the bottom of a mounting plate with a u-shaped stainless steel clasp. The fiber (yellow) coming from outside of the cryostat will then enter the filter bench on one side, and exit it on the other through an optical fiber leading to the TES.

3 Measurements and observations

In the following Section experiments have been conducted to test the filter's performance at cryogenic temperatures. At first the measurements conducted with THORLABS DET100A/M Si Biased Detector 400-1000 nm diodes [13] during cool-down and warm-up to examine the transmission of the beam will be discussed. Furthermore the spectrum of the laser before and after passing through the filter bench is being analyzed in a warm, as well as a cold environment. Lastly the observations made regarding the transmission will be compared with a theoretical simulation regarding the thermal expansion coefficient of the coupler materials.

3.1 Observation of laser power transmission

In order to examine the filter bench's behavior in a usual test run environment, its behavior is screened during one cool-down and warm-up cycle inside the cryocooler. In order to view the stability of the laser power and the behavior of the signal coming from the filter at the same time, a GOULD Fiber Optics [14] beam splitter was used to split the beam coming directly from the laser. It has four outputs only two are used in this setup. The input beam is split into four parts of approximately equal power each when passing through the beam splitter. As can be seen in Figure 6 one beam is directly sent to a diode (diode 0 or channel 0) whereas the other one enters the cryostat, passes through the filter and finally reaches diode 1 (or channel 1).

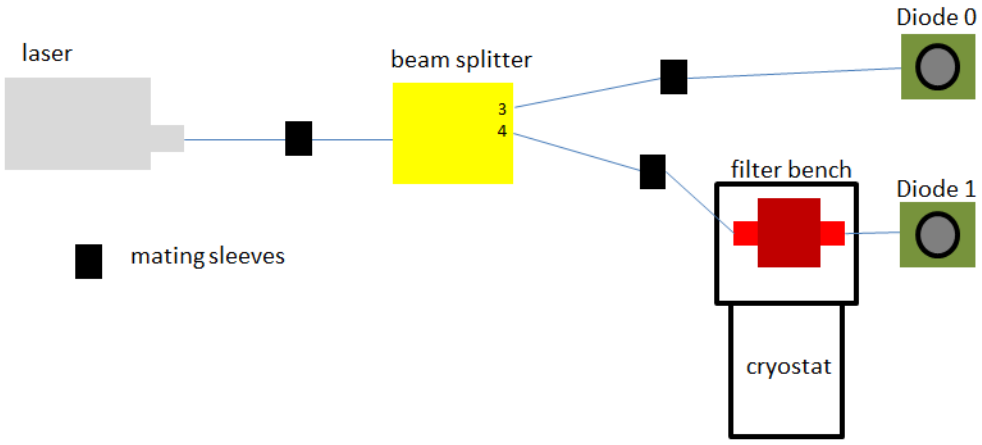

Figure 6: Setup for measuring the laser's power after passing through the filter bench. In this setup the filter bench includes one titanium and one nickel-silver coupler.

3.1.1 Cool-down

Figure 7 depicts the laser's behavior during the cool-down.
Although the laser's power (CH0) shows some fluctuations, these are only minor in comparison. During the creation of the vacuum the laser's power transmitted through the filter bench (CH1) increases for a short time and then decreases during the cool-down process reaching a stable power transmission after some time, which seems to stay fairly constant. Small deviations in the laser's power can also be recognized in the behavior of the beam after the filter. Although, as opposed to observations in [15] these are not always inverted during cool-down.
When looking at the ratio of the two channels with respect to the time and temperature as in Figure 9 a small drop and subsequent increase can be seen at what accounts for $\sim 150\,\mathrm{K}$. As of yet the reason for this cannot be discussed, since further measurements are needed to check if this behavior repeats itself. Through the shrinkage of filter bench material inside of the cryostat during the cool-down, an initial transmission of $\sim 66\%$ drops to $\sim 14\%$. This drop in transmission of almost 80% is far more than the drop of $\sim 30\%$ observed in [15]. This significant difference is most likely due to the different filter setup in comparison to the previous work. Due to problems with one of the titanium couplers, it had to be replaced with a nickel-silver coupler, which has a slightly higher thermal expansion coefficient and thus shrinks more than titanium. This will be discussed further in Section 3.3. Generally most of the shrinkage and thus transmission loss happens between $100\,\mathrm{K} - 200\,\mathrm{K}$. Beyond these temperatures the transmission seems mostly stable.

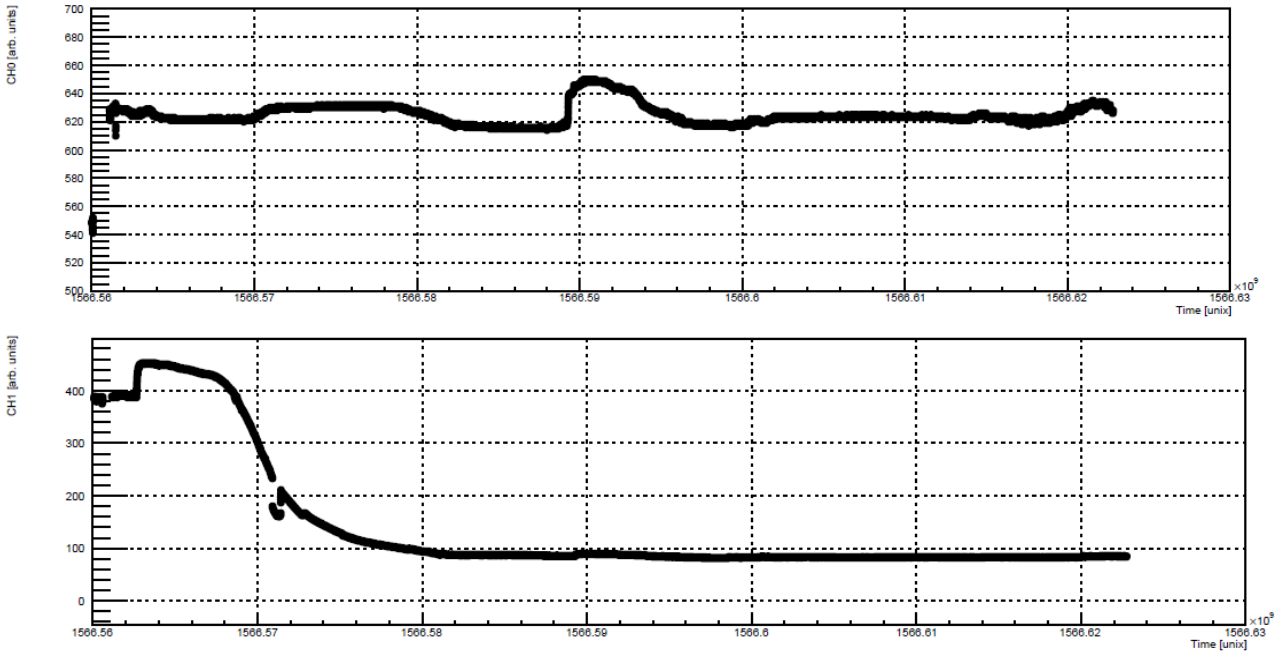

Figure 7: Laser behavior during cool-down:
Top: CH0, laser power over time (both in arbitrary units).
Bottom: CH1, filtered laser power over time (both in arbitrary units).

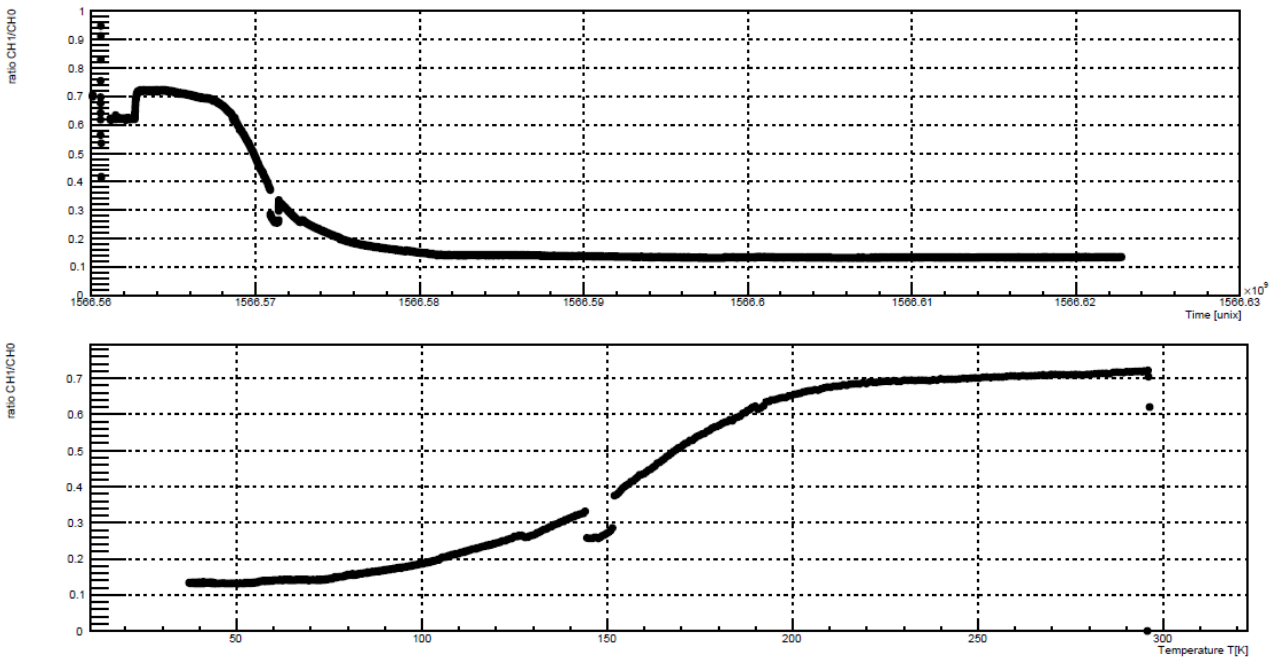

Figure 9: Ratio of transmitted laser power through the filter in regard to:
Top: time.
Bottom: temperature.

3.1.2 Warm-up

Figure 10 depicts the laser's behavior during warm-up.

Again the laser's power shows only slight fluctuations, which are to some degree visible in the filter's plot as well. Disregarding the rise in transmission, which in itself proceeds stably, the laser power

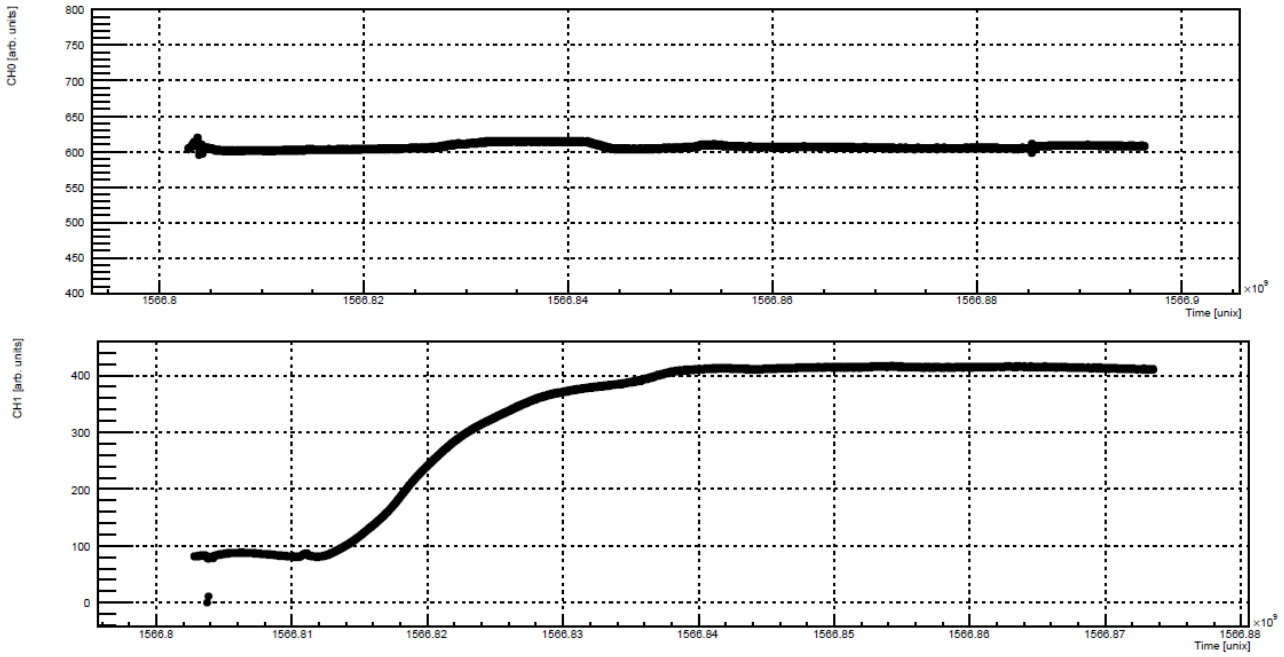

Figure 10: Laser behavior during warm-up:
Top: CH0, laser power over time (both in arbitrary units).
Bottom: CH1, filtered laser power over time (both in arbitrary units).

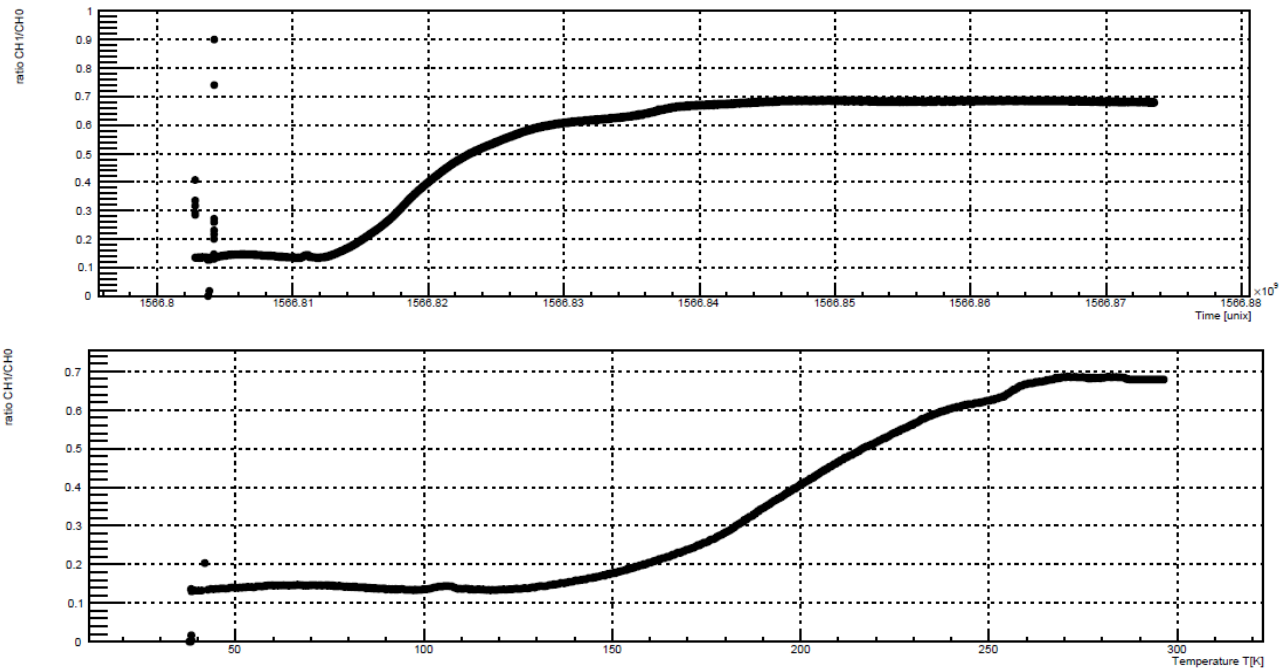

Figure 11: Ratio of transmitted laser power through the filter in regard to:
Top: time.
Bottom: temperature.

after the filter rises to its initial value and remains stable.
When taking another look at the ratios of the two channels in relation to time and temperature in Figure 11 it is visible that the reverse process happens slightly different. Since the ratio of the two channels with respect to the time rises back up to $\sim$ 66% and the process seems to be reversible,

the filter bench materials expand back to their original size and the initial alignment is thus restored. Interestingly, the expansion process seems to start later than during the cool-down. While the transmission stopped decreasing at $\sim$ 100 K during the cool-down, it only starts increasing significantly after $\sim$ 150 K during the warm-up. Whereas the transmission stayed constant until $\sim$ 200 K during cool-down it only reaches constant transmission after 250 K. Thus it seems that the shrinkage or expansion process takes some time to be initiated independent of the exact temperature measured at that moment. It should be mentioned additionally, that the measured temperature is not the temperature of the filter bench itself, but of a region slightly above its position in the cryostat. Thus it needs to be taken into account that it probably takes the filter bench longer to adjust to the temperature change. Another possible explanation for this could be limited thermal conductivity between the filter bench and the 40 K stage of the cryocooler, delaying the cooling process and thus the thermal shrinkage in that area. When the filter bench is placed in the cryostat the only means of providing thermal conductivity are the stainless-steel clamp and screws fixing the filter bench inside the cryostat.

Regardless, the behavior still poses interesting questions. If the drop in transmission, and thus the shrinkage of the material in cryogenic temperatures is this significant, then why does this only happen at certain temperatures and not below 100 K or above 250 K, also? The thermal expansion coefficient α is unique to each material, however it is not a constant but temperature dependent. It seems that below 100 K the material's shrinkage already "froze out", while the expansion significantly slows down above 250 K. As a consequence, another interesting behavior to be investigated is the change of the thermal expansion coefficient for titanium and nickel-silver in such a large low-temperature range.

3.2 Observation of laser spectrum

3.2.1 Warm environment

Before undertaking any spectrum measurements in cryogenic environment tests are carried out on the filter bench, including the new filter outside of the cryostat. At first the general spectrum of the 1064 nm laser was compared with the spectrum after the light passed through both the filter bench and the filter. The setup for this measurement can be seen in Figure 12. The spectra are recorded

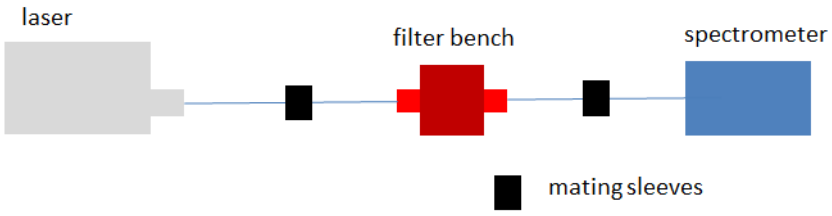

Figure 12: Setup for measuring the laser's spectrum after passing through the filter bench. For the measurement of the laser's spectrum itself, the laser was directly plugged to the spectrometers input. In this setup the filter bench still includes two titanium couplers.

with a SentroSpec 2048-VIS-NIR spectrometer and the getSoft version 7.0 software. First, the laser is run at 13 µW, which can be seen in Figure 13. This power was chosen since the spectrometer was already saturated at higher initial laser power and hence erroneous. Since the laser's maximum power is $\sim$ 300 µW this accounts for a small part of the laser's full power. Especially comparing this spectrum with one at maximum power, as in Figure 14, it is obvious that the laser's spectrum grows increasingly stable with growing power. In order to record these spectra without saturating the spectrometer the fibers going to the spectrometer were first plugged into an optical attenuator by Schäfter & Kirchhoff

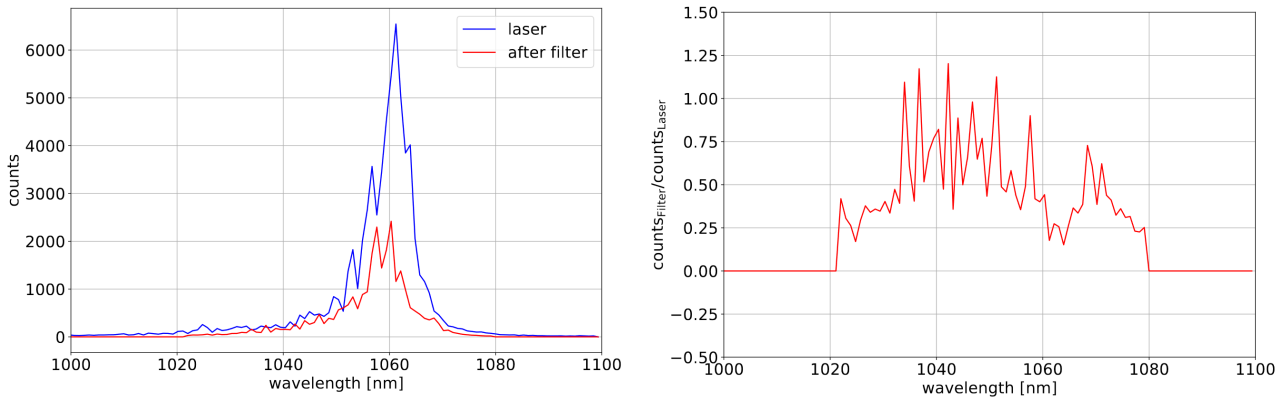

Figure 13: Left: Spectrum of the laser before and after passing through the filter bench. Right: Ratio of the counts recorded in the laser's spectrum before and after passing the filter bench; both at 13 µW initial laser power.

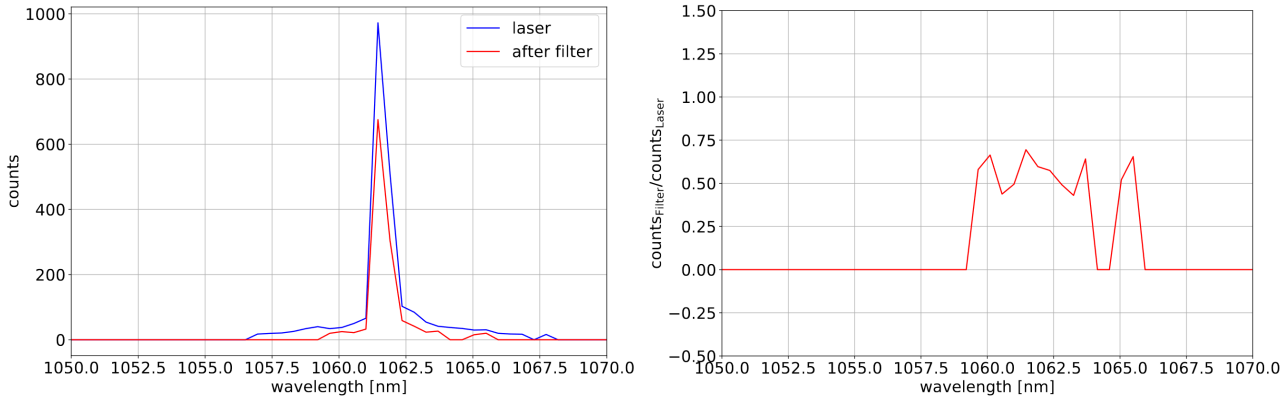

Figure 14: Left: Spectrum of the laser before and after passing through the filter bench. Right: Ratio of the counts recorded in the laser's spectrum before and after passing the filter bench; both at maximum laser power ($\sim$ 300 µW).

[11]. As already discussed in [15] the laser's spectrum does not peak at 1064 nm as opposed to its declaration. The main peak is positioned at $\sim$ 1061 nm.

Furthermore, it can be seen that the spectrum stays approximately the same after passing through the filter bench and bandpass filter. It does not seem as though wavelengths are shifted in the filtering process, which is in accordance with expectations. Since the filter's FWHM is 50 nm at a central wavelength of 1050 nm (see Section 2.2) the spectrum passing through the filter should not be influenced by it.

When calibrating the filter bench's couplers before measuring, the peak transmission usually reached $\sim 50\% - 70\%$ laser power through the filter bench with respect to the initial laser power. This is visible in the shown spectra, as well as the ratio plots. They also seem to be in accordance with the filter's properties approximately cutting out anything lower than 1020 nm and higher than 1080 nm for the noisy spectrum in Figure 13. Due to the laser's more stable signal in Figure 14 it seems as though the cutoff happens at an even smaller range, although this is probably due to the laser's slimmer and less noisy spectrum without any significant secondary peaks.

3.2.2 Cryogenic environment

Due to the laser's more stable performance at higher power an attenuator was permanently added to to the setup for the following measurements. The aim of this measurement is again to compare the laser's spectrum going into the cryostat with the spectrum coming out of the cryostat after passing through the filter bench in a cryogenic environment. As can be seen in Figure 15 the beam is split by the beam splitter: one beam is then sent to the spectrometer through the attenuator, while the other enters the cryostat, passes the filter bench and reaches the spectrometer through the attenuator. It is to be noted, that the used spectrometer has only one input, thus the measurements were never

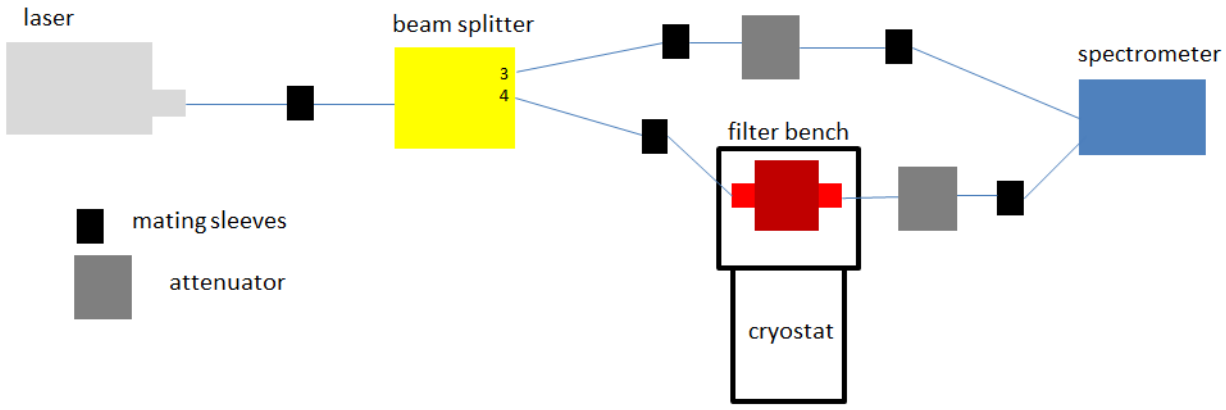

Figure 15: Setup for comparing the laser's spectrum with the spectrum after passing through the filter at cryogenic temperatures. In this setup the filter bench comprises of one titanium and one nickel-silver coupler.

performed simultaneously, but the different fibers coming from the beam splitter and the cryostat were directly plugged into the attenuator, instead. Another change was made on the filter bench in this setup: due to problems with one of the titanium couplers it had to be exchanged by a nickel-silver coupler, with the same setup as in Section 3.1.

At first, a spectrum was recorded before closing the cryostat and initiating the cool-down. The results are depicted in Figure 16. It should be noted again, that not only the attenuator decreases the signal

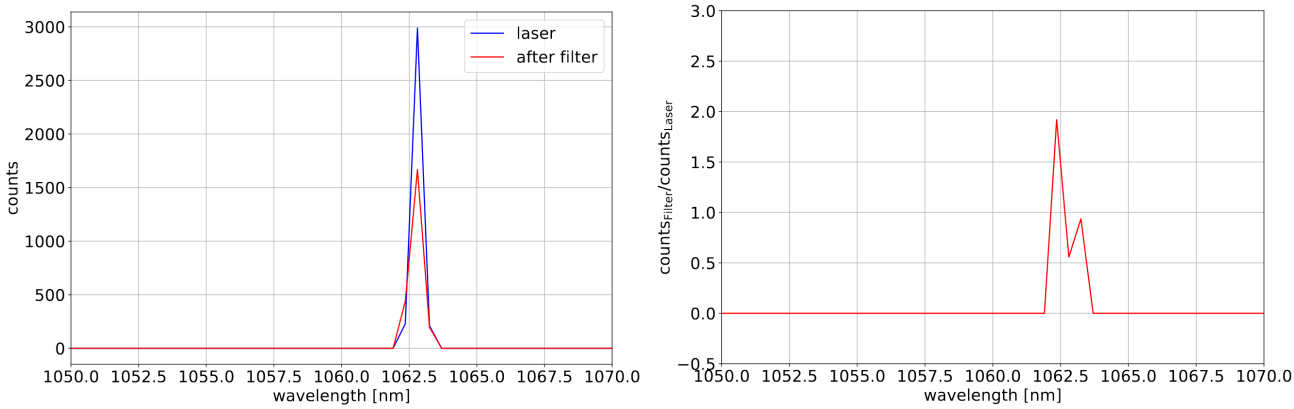

Figure 16: Left: Spectrum of the laser before and after passing through the filter bench. Right: Ratio of the counts recorded in the laser's spectrum before and after passing the filter bench; both at maximum laser power.

coming from the laser, but the beam splitter decreases the power as well.

When comparing this spectrum to the one from Figure 14, the peak intensity has shifted to a higher wavelength of $\sim 1063\,\text{nm}$. This could be traced back to a possible influence of the beam splitter and/or attenuator, since it is the main mechanical additional parameter that changed in comparison to Section 3.2.1. The spectrum coming from the filter still behaves in accordance to expectations and follows the recorded laser spectrum with lower intensity.

The same behavior as seen in Figure 14 can be seen in Figure 16, where it seems as if the cut-off region is shrinking, though this is due to the less noisy laser spectrum. The ratio of the power after and before the filter is strangely larger than one left of the main peak. In conjunction with this it is important to note, that the spectra were not taken at the same time, but successively; and the spectra showed a significant amount of fluctuation when recorded with the SentroSpec spectrometer. On the left hand side of Figure 16 the laser power after the filter slightly surpasses the laser power at a certain wavelength, which yields to the counter-intuitive depiction of the ratio on the right-hand side. This is suspected to be just a fluctuation in time.

After closing the cryostat and completing the cool-down cycle, which is when the lowest part of the cryostat has reached 40 mK, another set of spectra was recorded, which can be seen in Figure 17. The

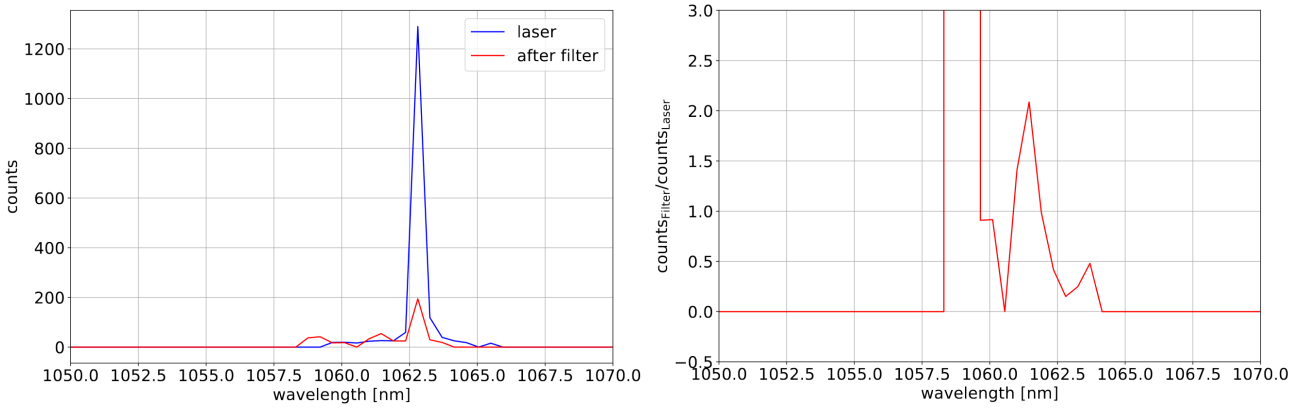

Figure 17: Left: Spectrum of the laser before and after passing through the filter bench. Right: Ratio of the counts recorded in the laser's spectrum before and after passing the filter bench both at maximum laser power at $T = 40\,\text{mK}$.

first major difference of the spectrum in comparison to the one after the cool-down is the number of counts in this spectrum. Even the laser's spectrum has decreased by more than half in comparison to Figure 16, even though nothing of that setup changed, since this part of the measurement always happened in the warm aka room temperature. Especially when comparing this to the intensity measured with the diodes (see Section 3.1), it is evident that the attenuator, which is only used for the measurements with the spectrometer, has some influence on the low spectrum coming from the laser.

As expected from the diodes' measurements the transmission of the main peak is not very good and drops to $< 20\%$ of initial power. As explained in Section 3.1, this is most likely due to thermal shrinkage of the filter bench material, which changes the optical properties of the setup. Furthermore the spectrum does not seem to be as stable, in comparison to the one coming directly from the laser, although these might be mere fluctuations. This also influences the two spectra's ratios, since the intensity of the spectrum coming from the filter seems to be larger than the original spectrum in some places. Anyhow the cut-off is still visible, although the information value of this plot is questionable.

To further discuss the issue: From Section 3.1 it is evident that the laser's power has been approxi-

mately stable throughout the whole cool-down and even warm-up process, so the behavior measured by the spectrometer does not match this observation. This leads to the conclusion, that something in this measurement's setup influences the spectrum, which yields these deviations. Since the additional parameter is the attenuator, this, perhaps in interplay with the beam-splitter, seems to be the source for this behavior. When conducting tests on the attenuator after completion of the warm-up process the behavior seems to be even more contrary, as can be seen in Figure 18.

Although when checking the diodes the laser's intensity is still stable before and after this measure-

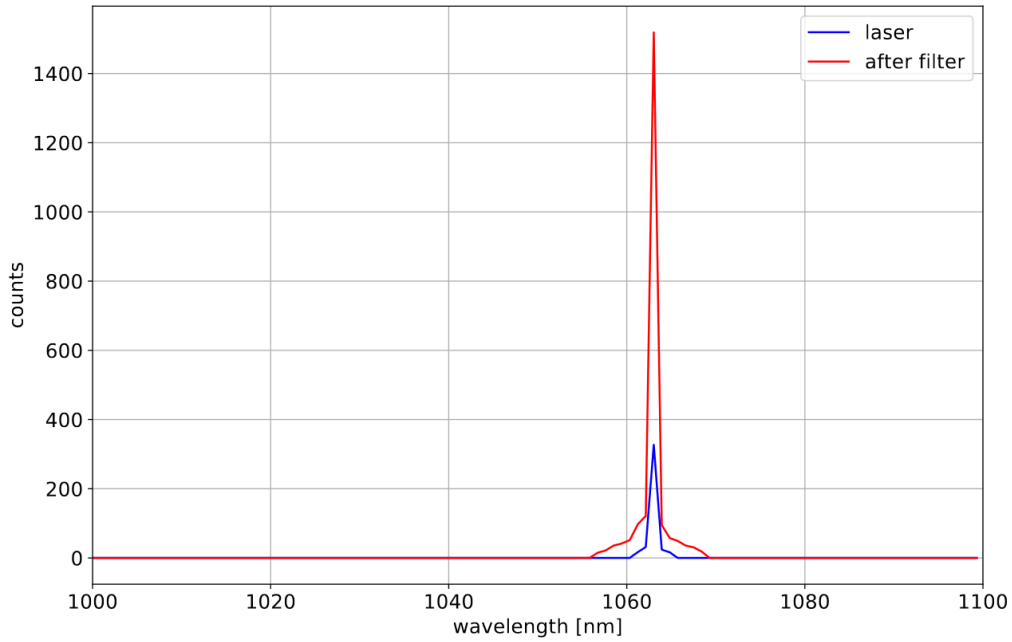

Figure 18: Spectrum of the laser before and after passing through the filter after warm-up with presumably faulty setup, since the power after the filter far surpasses the laser's initial power. This is in direct contradiction of the power measurements conducted with the diodes.

ment. Thus the laser power before and after the attenuator was measured for both the laser and the beam after the filter. The results can be seen in table 1. This clearly shows, that even though the

	Laser	Filter
before attenuation	$\sim 30\,\mu W$	$\sim 23\,\mu W$
after attenuation	$\sim 100\,nW$	$\sim 400\,nW$

Table 1: Influence of the attenuator on transmitted laser power.

laser's power transmitted to the attenuator is higher than the one first passing through the filter bench, it is dampened more by the attenuator than the lower signal coming from the filter, explaining the contrary behavior in Figure 18. There are multiple possible reasons for this. For example, the beam splitter could be not splitting the beams in four equal parts but could dampen the spectrum more or less in some parts depending on the used output. Another possibility is the influence of the multiple mating sleeves used in this setup on the laser's spectrum. All of these will need to be investigated further in the future.

3.3 Comparison with expectation from thermal expansion coefficient

In [15] it has already been discussed that the main reason for the drop in transmittance might be the thermal shrinkage of the filter bench's couplers. One solution to tackle these losses could be to purposefully misalign the couplers and thus the optical fibers to avoid the transmittance loss, however this poses a high risk of misaligning the setup even more and in order to do this it is of prime importance to understand the behavior of the filter bench's materials at cryogenic temperatures and to evaluate whether the transmission losses are actually the result of thermal material shrinkage.

To compare which amount of material shrinkage accounts for how much loss in transmission, calculations were made by Elena Mazzeo (2018) in a simulation which is described in detail in [15]. Figure 19 shows the transmittance t of a system in relation to the distance of an optical fiber from a parallel light source. At first the expected thermal shrinkage for the current experimental setup is

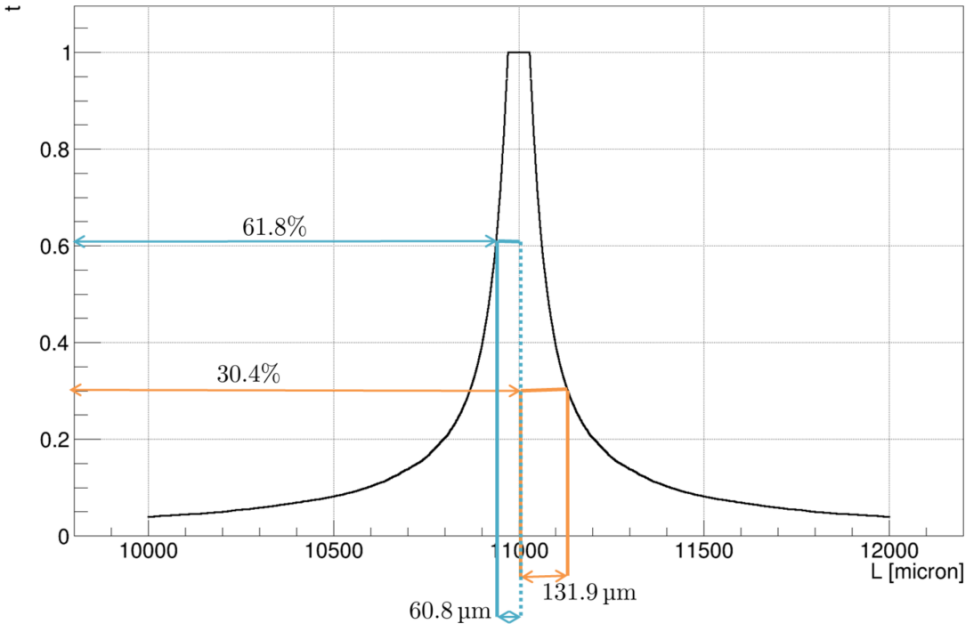

Figure 19: Transmittance of a simulated setup as a function of the distance L between lens and optical fiber. The orange line accounts for the transmission with a nickel-silver coupler, the blue line for a titanium coupler. Plot adapted from [15].

calculated. When repeating the calculations done in [15], but one for a nickel-silver coupler with a coefficient of thermal expansion of $\alpha_{\mathrm{NS}} = 18.4 \cdot 10^{-6}\,\mathrm{K}^{-1}$ [16] (approximation at room temperature), this yields an expected shrinkage of the coupler of $\Delta l_{\mathrm{NS}} = 131.9\,\mu\mathrm{m}$. The expected thermal shrinkage of the titanium coupler is $\Delta l_{\mathrm{T}} = 60.8\,\mu\mathrm{m}$ with a thermal expansion coefficient of $\alpha_{\mathrm{T}} = 8.5 \cdot 10^{-6}\,\mathrm{K}^{-1}$[15].

The thermal shrinkage of one coupler brings the coupler and an optical fiber closer together, reducing the distance L in the simulation. Thus the change in length can be plugged into the simulation and compared with the amount of transmission this accounts for. For nickel-silver this yields for 30.4% transmission, whereas the transmission for titanium is much better with 61.8%. This yields for an overall transmission of $t_{\mathrm{all}} = t_{\mathrm{NS}} \cdot t_{\mathrm{t}} = 19\%$. When comparing this to the transmission loss witnessed in Section 3.1 the transmittance loss from 66% to 14% accounts for a transmission window of $\frac{0.14}{0.66} \approx 0.21$. Comparing this to the simulation it is evident that most of the transmission loss happened due to thermal shrinkage of the filter bench materials. The simulation even expected more transmission loss

to happen. That this is not the case is most likely due to the fact that the calculations were done with a constant value for the thermal expansion coefficient of both materials, when in fact thermal shrinkage/expansion is not a linear process, as is evident from Section 3.1 as well.[2] The calculations were done over the complete range of temperature change, even though we can see in Figure 10 that the process of thermal expansion only starts after a while. Thus this simulation is only an approximation.

4 Conclusions and Outlook

The filter bench with the new bandpass filter for the ALPS II TES group was successfully installed into the cryostat and tested during one cooling cycle. Its current setup is transparent to a spectrum in the range from 1000 nm to 1100 nm, so the filter works as expected. However, there are still large losses in transmission of the laser beam. After calibration of the filter bench's fiber couplers a transmission of 66% in the warm was reached. After one cooling cycle the transmission dropped as low as 14% although this has been reversible during the warm-up, after which a transmission of $\sim 66\%$ was achieved again. The laser that has been used for these measurement shows some inconsistencies in the spectrum regarding the wavelength of its main peak, thus this behavior will need to be examined further regarding the different setups and components therein such as beam splitter, attenuator and mating sleeves.

In examining the laser's spectrum during the cool-down as well, the same behavior as in the diode measurement has been observed, where the transmission dropped significantly. This is presumably mostly due to thermal shrinkage of the filter bench material. Especially the currently used nickel-silver coupler accounts for most of the losses in transmission as has been proven by a simulation of the used setup. The simulation, using the thermal expansion coefficient of the used materials, predicts an overall transmission of $\sim 19\%$, whereas the current setup shows an overall transmission of $\sim 21\%$, clearly showing a dependency of the laser transmission on the mechanical properties of the used materials. Thus this behavior should be characterized further and two titanium couplers should be used again in order to reduce transmission loss. In using two titanium couplers the expected transmission would already rise from $\sim 18\%$ to $\sim 38\%$, showing that this should be taken into consideration.
In conclusion the filter shows promising properties for future testing, also regarding background tests with the TES to achieve first results on its efficiency in reducing black body pile-up.

[2] Furthermore the values for the thermal expansion coefficient are not constant over the whole temperature range, although we assumed they were.

5 References

[1] *R. Peccei & H.R. Quinn*, CP conservation in the presence of instantons, (1977). Phys.Rev.Lett., 38:14401443.

[2] *J. Dreyling-Eschweiler*, A superconducting Microcalorimeter for Low-Flux Detection of Near-Infrared Single Photons, U. Hamburg, Dept. Phys., desy-thesis-14-016.

[3] *M. Meyer et. al.*, First lower limits on the photon-axion-like particle coupling from very high energy gamma ray observation, (2013). Phys.Rev.,D87:034027. arXiv: 1302.1208.

[4] *P. Gondolo & G.G. Raffelt*, Solar neutrino limit on axions and keV-mass bosons, (2009). 79(10):107301.

[5] *K. Ehret et.al.*, Resonant laser power build-up in ALPS - A light shining through a wall experiment, (2009). NUclear Instruments and Methods in Physics Research Section A: Accelerators Spectrometers, Detectors and Associated Equipment, 612(1):83-960.

[6] *K. Ehret et al.*, New ALPS results on hidden-sector lightweights, Physics Letters B 689 (2010) 149155, doi:/10.1016/j.physletb.2010.04.066 .

[7] *R. Hodajerdi*, Optics for a Light Shining through a Wall Experiment, U. Hamburg, Dept. Phys., 10.3204/DESY-THESIS-2015-005.

[8] *NIST*, `https://www.nist.gov/`[Accessed 30.08.2019].

[9] *BlueFors*, `https://bluefors.com/products/sd-dilution-refrigerator/` [Accessed 30.08.2019].

[10] *Edmund Optics*, `https://www.edmundoptics.de` [Accessed 31.08.2019].

[11] *Schäfter & Kirchhoff*, `https://www.sukhamburg.com/produkte.html` [Accessed 31.08.2019].

[12] *K. Zenker*, Construction of a filter bench for ALPS. Internal communication 2017.

[13] *THORLABS*, `https://www.thorlabs.com/index.cfm` [Access 04.09.2019].

[14] *GOULD Fiber Optics*, `https://gouldfo.com/` [Accessed 02.09.2019].

[15] *E. Mazzeo*, The challenge of filtering photons in a cold environment, University of Milan, DESY 6.9.2018, ALPS.

[16] *Engineering ToolBox*, (2003). Coefficients of Linear Thermal Expansion. `https://www.engineeringtoolbox.com/linear-expansion-coefficients-d_95.html` [Accessed 30.08.2019].